

Modeling and Simulation of Temperature Generated on Workpiece and Chip Formation in Orthogonal Machining

Hendri Yanda, Jaharah A. Ghani, Che Hassan Che Haron

Abstract – Experimental investigation in machining operation for the temperature generated on workpiece, chip formation and cutting tool are difficult, time consuming and costly to carry out. Machining simulation using FEM software is an alternative. This paper presents a simulation study of temperature generated on workpiece and chip formation for various combinations of tool geometries (rake angle and clearance angle). Ductile cast iron FCD500 grade was used as material workpiece, and uncoated carbide tools with code number DNMA432 were used as cutting tool. Twelve designs of carbide cutting tools with various combination of rake angle (15, 20, and 30 deg) and clearance angle (5, 7, 8 and 9 deg) were designed. The nose radius of the cutting tool was kept constant at 0.4 mm. Machining parameters of cutting speed, feed rate and dept of cut (DOC) were kept constant at 200 m/min, 0.35 mm/rev and 3 mm respectively. Using a commercial software package Deform-3D, twelve orthogonal machining simulations were carried out to analyze the effect of tool geometries on temperature generated and chip formation. The results show that by increasing the rake angle, the machining performance is improved due to the low temperature generated on the machined surface, as well as low cutting force, stress, and strain. On the other hand, increasing/decreasing the clearance angle, does not significantly affected the cutting force, stress, and strain, consequently it does not affected the temperature generated. For the chip formation, the highest temperature occurred in the sliding region due to the work piece material adheres to the cutting tool and shear occurs within the chip, the frictional force is very high; consequently heat is generated from this sticking region

Keywords: carbide tool, chip formation, cutting force, generated temperature, tool geometry.

I. Introduction

To understand the physical phenomena generated during cutting processes, the characterization of the temperature field is essential, because the most important part of the work generated during the cutting process is converted into heat [1].

There are three main regions concerned with heating during the cutting process: the primary shear zone where the chip is formed and characterized by high shear deformation. The secondary and the tertiary zone where friction and shearing are combined are located respectively along the tool-chip interface and below the tool edge. In these regions heat is generated and flows into the workpiece, chip and cutting tool.

The energy required to deform the workpiece material and the chips is mainly converted into heat. As shown in Fig.1, there are three zones in which the heat is generated [2]:

- Primary deformation zone; where plastic deformation takes place and Q_S is generated.

- Secondary deformation zone; where the deformation takes place in the tool-chip interface and as the result of friction force, Q_C occurs.
 - Tertiary deformation zone; where the heat is generated due to friction between tool clearance face and newly generated workpiece surface, Q_F .
- Thus, the total heat, Q_T can be obtained by the following Eq. (1) [2].

$$Q_T = Q_S + Q_C + Q_F \quad (1)$$

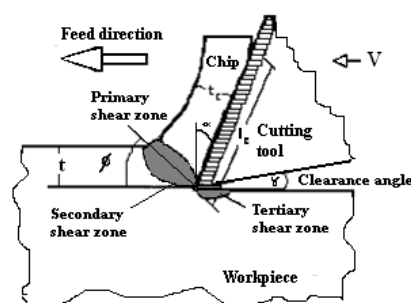


Fig. 1. Generation of heat in orthogonal cutting

The machining problems of cast iron have been not necessary foundry-related, but most of problem were due to the microstructure formation during the machining process itself. According to Jaharah et al [3], the width of microstructure changes, increases with the increase in wear land and feed rate. Therefore, study on the machinability of ductile cast iron is required to improve the productivity as well as to obtain the optimal machining parameters.

The temperatures, and also the effective stress generated on the cutting edge, are affected most by cutting speed, followed by feed rate and tool geometries [4]. Controlling the generated temperature is also important in maintaining and controlling the microstructure and hardness underneath workpiece's surface [5]. In addition the worn tools caused overheating in the machined surface, resulting in changes to the microstructure of the work material.

The temperature is also an important parameter controlling to tool wear and consequently the tool life, the quality of the surface finish, chip segmentation and the choice of lubrication. Furthermore, thermal aspects become more important with high cutting speeds used presently in industrial processes.

A large number of techniques [6] have been developed to quantify the temperature, which can be classified as intrusive (e.g. thermocouple technique [9] or non-intrusive techniques (e.g. pyrometry technique [10]-[12]). Most of the above mentioned experiments are expensive, high risk and time consuming, therefore as an alternative, machining simulation is suggested. By performing the machining simulation, problems related to high cost, time, and injuries caused by high temperature and other high risks in machining experiments can be prevented.

This paper presents the application of FEM simulation to predict the effect of tool geometries (rake angle and clearance angle) on temperature generated on workpiece and chip formation.

II. Literature Review

II.1. Temperature Measurement Techniques

The heat generated in cutting is one of the most important topics investigated in machining. There are several experiment techniques that have been developed by many researchers before for the measurement of temperature in various machining processes and manufacturing applications. Some of the techniques can be categorized as: (1) Calorimetric [13][14] (2) thermocouples [15], (2) infra-red photography [16][17]; (3) optical infrared radiation pyrometers [18], and others. All of experiment techniques required high cost and time.

The second highest heat generated was occurred on the tool-chip formation interface as shown in Fig.1. The ingenious method of determining the partition of heat generated in cutting between the tool, the workpiece, and the chip can be decided by previous researcher [19]. Fig. 2 shows a typical distribution of heat in the workpiece, the tool, and the chips with cutting speed [17].

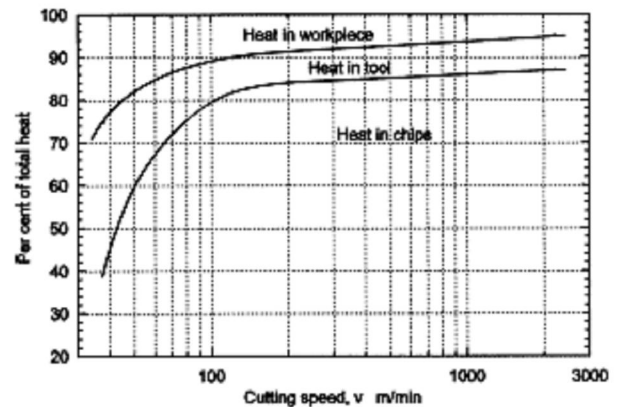


Fig. 2. Typical distribution of heat in the workpiece, the tool, and the chips with cutting speed [17]

II.2. Finite Element Analysis (FEA) Technique

Finite Element Analysis (FEA) technique was first introduced in 1960s and has been widely used in designing tools and forming processes. Based on the success of FEM simulations for bulk forming processes, many researchers developed their own FEM codes to analyze metal cutting processes during the early 1980s up to now [20]-[25].

A rigid sharp tool and elasto-plastic workpiece, and defined a node separation criterion based on the geometry of the element approaching the edge of cutting tool were assumed [21]. An early version of a commercial implicit FEM code Deform-2D™ was used [21]. This code uses four-node quadrilateral elements and is based on a static Lagrangian formulation. Scientific Forming Technologies Corporation [26] introduced Deform-3D™ code that has been commonly used by researchers and industry for machining simulation.

Applications of FEM models for machining can be divided into six groups: a) tool edge design, b) tool wear, c) tool coating, d) chip flow, e) burr formation and f) residual stress and surface integrity. The direct experimental approach to study machining processes is expensive and time consuming. For solving this problem, the finite element methods are most frequently used.

Modeling tool wear using FEM has advantages over conventional statistical approach because it requires less experimental effort and it provides useful information

such as deformations, stress, strain and temperature in chip and the workpiece, as well as the cutting force, tool stress and temperature on the tool working under specific cutting parameter [27].

II.3. Heat Transfer

The sources of heat generation are the plastic work in the cutting zone and friction at the tool–chip interface. At the same time, workpiece loses heat to the environment due to convection and to tool due to conduction. The rate of specific volumetric flux due to plastic work is given by Eq. (2).

$$\dot{q} = \frac{\zeta \cdot \kappa \cdot W^P}{\rho} \quad (2)$$

Where W^P is the rate of plastic work, κ is the fraction of plastic work converted into heat, ζ is the mechanical equivalent of heat and ρ is the density of workpiece material.

The rate of heat generated due to friction is given by Eq. (3).

$$\dot{Q} = F_{fr} \cdot v_r \cdot \zeta \quad (3)$$

where F_{fr} is the friction force, v_r is the relative sliding velocity between tool and chip, and ζ is the mechanical equivalent of heat. The generated heat due to friction is given to each of the two contacting bodies, which are chip and tool in this case, by equal proportions.

The workpiece loses heat to the environment due to convection according to Eq. (4).

$$q_h = h \cdot (T_w - T_o) \quad (4)$$

where h is the convection heat transfer coefficient of the workpiece, T_w is the workpiece surface temperature, and T_o is the ambient temperature.

III. Modeling and Simulation of Generated Temperature

III.1. Machining Parameter

Twelve runs of simulation were conducted for various design of rake angles of 15, 20, and 30 deg, and clearance angles of 5, 7, 8, and 9 deg, while nose radius was kept constant at 0.4 mm. The machining parameter, such as cutting speed, feed rate and depth of cut, were

kept constant at 200 m/min, 0.35 mm/rev and 0.3 mm respectively as shown in Table I.

TABLE I
INPUT PARAMETERS IN THE SIMULATION PROCESS

Parameters	
Cutting speed	Kept constant at 200 m/min
Feed rate	Kept constant at 0.35 mm/rev
Depth of cut	Kept constant at 0.3 mm
Nose radius (r_n)	Kept constant at 0.4 mm
Rake angle (α)	15, 20 and 30
Clearance angle (β)	5, 7, 8 and 9

III.2. Material Properties and Simulation Modeling

Fig.3 shows the geometry and schematic of orthogonal cutting condition model for the rake angle of 15 deg and clearance angle of 7 deg.

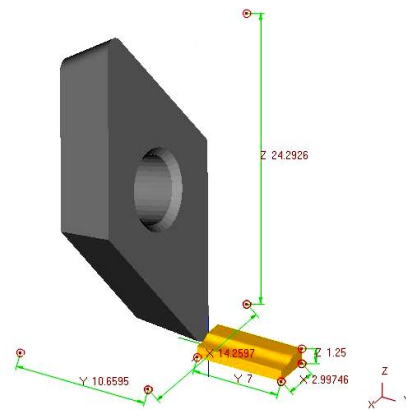


Fig. 3. Geometry and schematic of the orthogonal cutting condition model for rake angle of 15 deg and clearance angle of 7 deg

TABLE II
COMPOSITION OF CAST IRON FCD500 GRADE

Element	Percentage (%)
C	2.77
Si	1.26
S	0.11
P	0.036
Mn	1.24
Ni	0.26
Cr	0.27
Mg	0.09
Cu	0.18
Mg	0.127
Al	0.063
Co	0.073

Source: Sirim, 2008

TABLE III
FLOW STRESS MODELS USED IN SIMULATION

Material Model	Equation for flow stress σ models	Material constants	Variables
Oxley model	$\sigma = \sigma_1 \epsilon^n$	$\sigma_1, n = f(T_{mod})$	$\epsilon, \dot{\epsilon}, T$

TABLE IV
MECHANICAL AND THERMAL PROPERTIES AND BOUNDARY
CONDITION FOR THE SIMULATION MODEL

Tool geometry of DNMA432 (WC as base material, uncoated tool)	
Rake angle, α (deg)	15, 20 and 30
Clearance angle, β (deg)	5, 7, 8 and 9
Cutting corner radius, (r_ϵ) (mm)	0.4
Tool properties	
Modulus Young (GPa)	650
Modulus of elasticity (GPa)	641
Poisson ratio	0.25
Boundary condition	
Initial temperature ($^{\circ}\text{C}$)	20
Shear friction factor	0.6
Heat transfer coefficient at the workpiece-tool interface ($\text{N/s. mm}^{\circ}\text{C}$)	45
Workpiece geometry (ductile cast iron FCD500 grade)	
Depth of cut	0.3
Width of cut (mm)	3.4
Length of workpiece	10
Workpiece properties (Ductile cast iron FCD500; Poisson's ratio, 0.275)	
Modulus elasticity (GPa)	169
Thermal conductivity ($\text{W/m. }^{\circ}\text{C}$)	35.2
Thermal expansion Coefficient ($\cdot 10^{-6} \text{ }^{\circ}\text{C}^{-1}$)	12.5
Heat capacity ($\text{N/mm}^2 \text{ }^{\circ}\text{C}$)	3.7
Emissivity	0.95
Others	
The fraction of plastic work conversion into heat, κ	0.9
Mechanical equivalent of heat, ζ	1.0
Density (g/cm^3)	7.875
Convection heat transfer coef., $\text{N/(mm }^{\circ}\text{C)}$	0.4

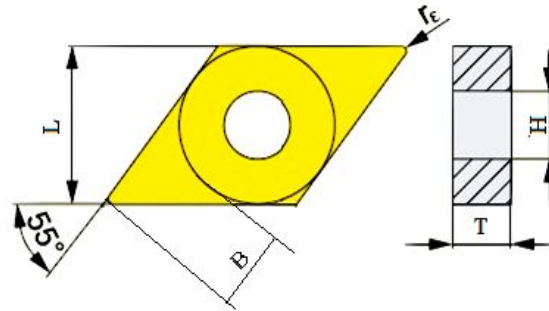
The work piece was ductile cast iron FCD500 grade and the cutting tool used was code number DNMA432 (tungsten, uncoated carbide tool, SCEA= 0; nose radius = 0.4mm, and nose radius angle 55°). This material was chosen as the workpiece material in this study because it was widely used in automotive component. Table II shows the composition of ductile cast iron FCD500 grade. The flow stress model used was the equation given by Oxley [9] as shown in Table III.

In these simulations, the tools were defined to be an elastic body and isothermal, so the mechanical and thermal properties and also boundary condition for simulation model are given in Table IV.

III.3. Design of Cutting Tool Geometries

Cutting tools were designed for various positive rake angles of 15, 20 and 30 deg and the clearance angles of 5, 7, 8 and 9 deg, while nose radius was kept constant at 0.4 mm. Geometries of tool carbide with code number DNMA432 can be seen in Fig.4.

Table V shows the variation of tool geometries where there are four clearance values for each rake angle. The twelve combinations of tool geometries were designed using Solid Work software as shown in Fig 5b, 5c, and 5d. The schematic diagram of cutting tool geometries is shown in Fig. 5a.



DNMA432: IC = 12 mm, T = 4.76, B= 6.5, and H=5.2

Fig. 4. Geometries of tool carbide with code number DNMA432 [26]

TABLE V
VARIATION OF CUTTING TOOL GEOMETRIES

Rake Angle (α)	Clearance Angle (β)	Nose radius, (r_ϵ)	Nose angle
deg	deg	mm	deg
+15	5, 7, 8 & 9	0.4	55
+20	5, 7, 8 & 9	0.4	55
+30	5, 7, 8 & 9	0.4	55

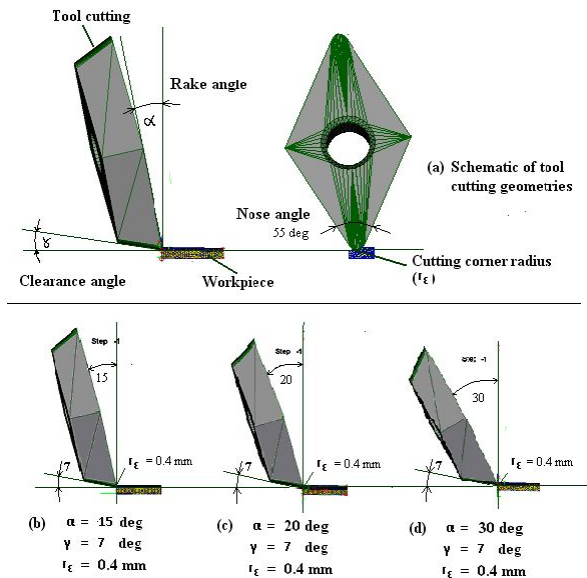


Fig. 5. (a) Schematic diagram of tool geometries; (b), (c), and (d) various designs of rake angles of 15, 20, and 30 deg, and clearance angle and nose radius were kept constant at 7 deg and 0.4 mm

III.4. Finite Element Models

The finite element model is composed of a deformable workpiece and a rigid tool. The tool penetrates through the workpiece at a constant speed and constant feed rate.

A 3D finite element model was developed using Deform-3D 6.1 finite element modeling software as shown in Fig. 6. The modeling approach is based on updated Lagrangian formulation for large plastic deformation analysis to simulate chip formation. The formation of chip from initial mesh (Fig. 6a) until it forms continuous chip at step 100, 200 and 500 (Fig. 6b, 6c and 6d respectively) were developed by 6170 number of elements and 1513 nodes for cutting tool, and 4746 number of elements and 1190 nodes for workpiece. The simulations were done in 500 step for transient condition and 500 steps for steady state condition (1000 steps in totally).

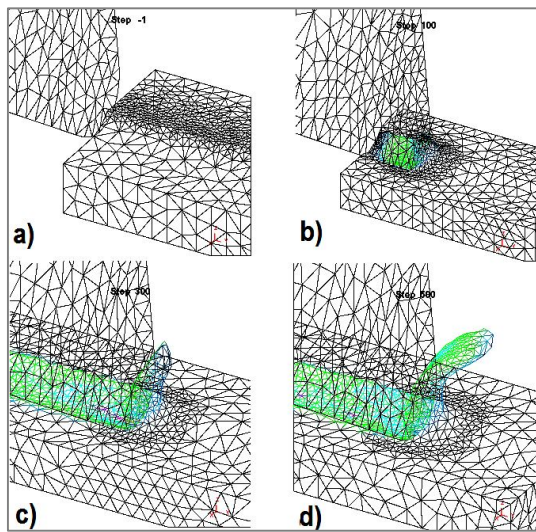


Fig. 6. (a) Initial mesh and tool indentation, (b) Chip formation at step 100, (c) Chip formation at step 200, (d) Developed continuous chip at step 500

The workpiece and the tool are characterized by non uniform mesh distribution in the simulation. Very small element (20% of feed or 0.06 mm) is required in the contact area between tool and workpiece because of very large temperature gradient and stress that will be developed in this region during the simulation.

Fig.7 shows an example of transient simulation result for rake angle of 15 deg and clearance angle of 7 deg, the cutting speed of 100 m/min, feed rate of 0.35 mm/rev and DOC of 0.3 mm, at 500 steps of simulation running.

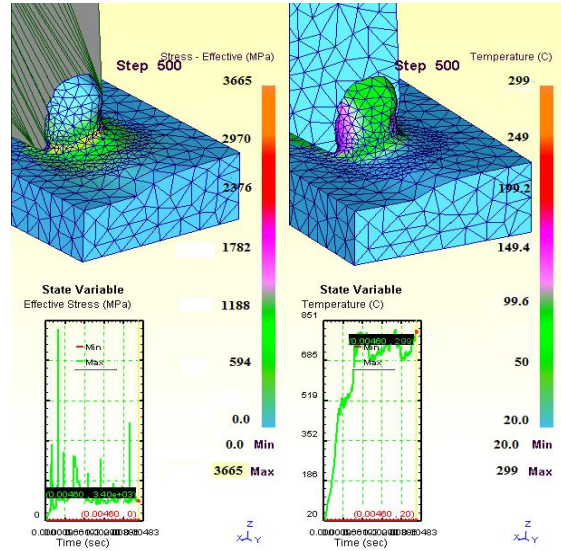


Fig. 7. Example of the transient simulation result for cutting speed of 200 m/min and rake angle of 15 deg and clearance angle of 7 deg (after running in 500 steps)

IV. Simulation Results and Discussion

Table VI shows the simulation results for all combination of various rake angles and clearance angles at cutting speed of 200 m/min, feed rate of 0.35 mm/rev and depth of cut (DOC) of 3 mm.

Table VI
THE RESULT OF SIMULATION FOR CUTTING FORCE, STRESS, STRAIN, AND TEMPERATURE

No	Rake angle, α [deg]	Clearance angle, β [deg]	Cutting speed, V [m/min]	Feed rate, f [mm/rev]	DOC, a [mm]	Temp, T [°C]	Cutting force, F_c [N]	Stress, σ [MPa]	Strain, ϵ [mm/mm]
1	15	5	200	0.35	3	321	346	4320	6.11
2	15	7	200	0.35	3	318	347	4230	6.56
3	15	8	200	0.35	3	334	400	4195	6.24
4	15	9	200	0.35	3	304	402	4340	7.13
5	20	5	200	0.35	3	299	239	3565	5.03
6	20	7	200	0.35	3	304	295	3690	4.96
7	20	8	200	0.35	3	272	271	3690	5.56
8	20	9	200	0.35	3	263	297	3720	5.65
9	30	5	200	0.35	3	198	165	3360	4.31
10	30	7	200	0.35	3	206	178	3540	4.45
11	30	8	200	0.35	3	218	196	3537	5.07
12	30	9	200	0.35	3	225	262	3400	4.68

IV.1. The Effect of Rake Angle (α)

By increasing the rake angle, the temperature generated, cutting force, stress, and strain are decreasing as shown in Fig. 8, 9, 10 and 11 respectively. For example, increasing the rake angle from 15 deg to 30 deg (clearance angle of 7 deg), will reduce the temperature generated on workpiece from 321 °C to 198 °C, the cutting force from 346 N to 165 N, stress from 4320 MPa to 3360 MPa, strain from 6.11 to 4.31 mm/mm.

This is due to the reason that by reducing the temperature, consequently reducing the cutting force, stress, and strain. The cutting force, stress, strain decreased because of the small tool/chip contact area. When increasing the rake angle, the contact area at the interface between the tool and workpiece will decrease. This is agreeable with theory and experiment done by [28].

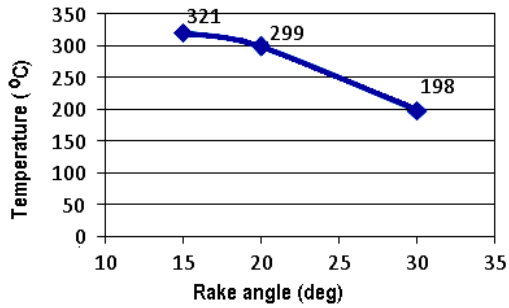


Fig.8. Rake angle vs Temperature

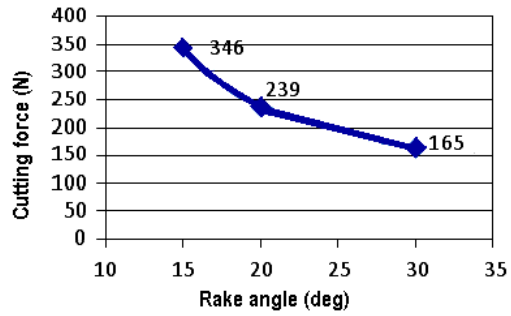


Fig. 9. Rake angle vs Cutting force

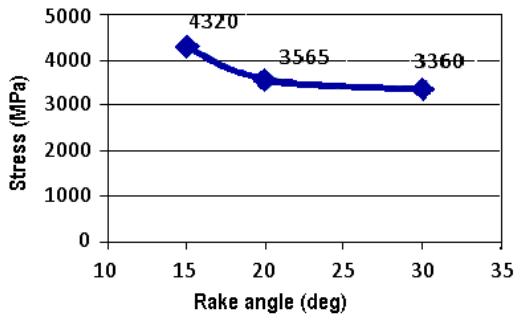


Fig. 10. Rake angle vs Stress

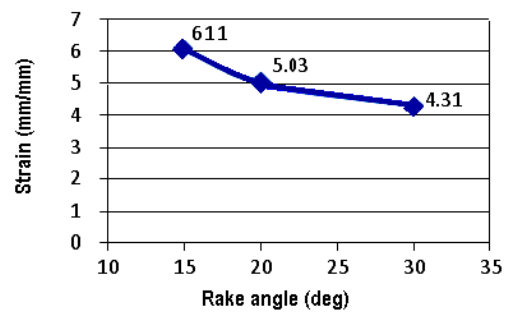


Fig. 11. Rake angle vs Strain

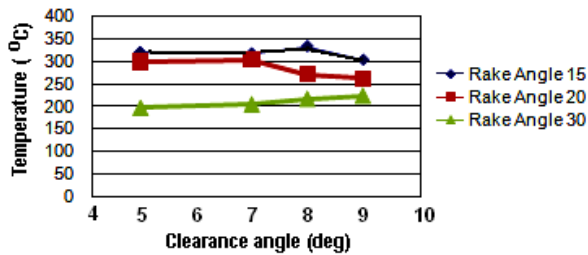


Fig. 12 Clearance angle vs Temperature

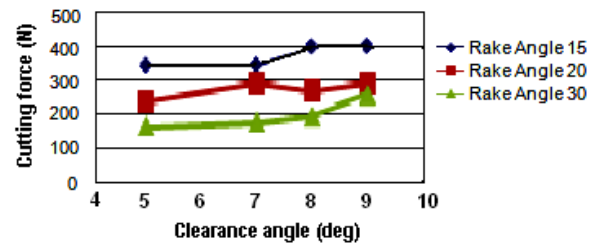


Fig. 13. Clearance angle vs Cutting Speed

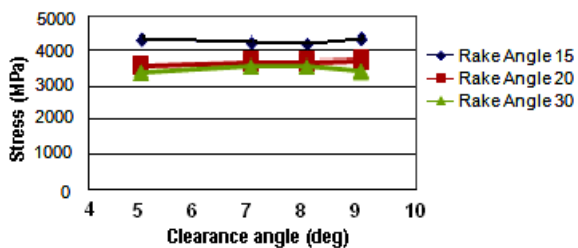


Fig. 14. Clearance angle vs Stress

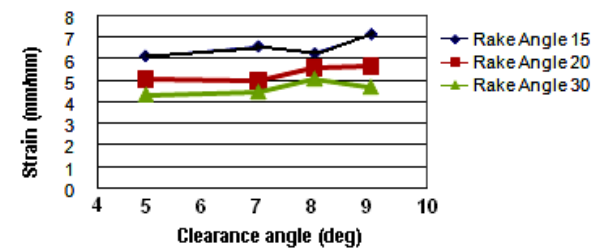


Fig. 15. Clearance angle vs Strain

IV.2. The Effect of Clearance Angle (γ)

Increasing the clearance angle does not much influence the temperature generated, cutting force, stress, and strain as shown in Fig. 12, 13, 14, and 15 respectively. All of these results were also agreeable with the theory [29], because the change of clearance angle will not affect the cutting force and stress, therefore the temperature generated on workpiece will not be affected.

The increase of clearance angle will slightly affects the wear rate. Clearance angle will affects wear and tool life of the cutting tool because it will rubs against the freshly cut metal surface. In industry, the clearance angle is varied, but often in the order of 6 – 10 deg [30].

IV.3. Chip Formation: Generated Temperature on Primary and Secondary Deformation Zone.

Heat generation in metal cutting process is primarily due to shear deformation of the work material during chip formation. The temperatures of the tool body, however, are mainly increased due to the heated chip passing over the chip-tool interface.

Fig. 16 shows the simulation results for temperature generated, displacement, stress, and strain for rake angle

of 20 deg and clearance angle of 5 deg (cutting speed of 200 m/min, feed rate of 0.35 mm/rev and DOC of 3 mm).

The highest temperature of about 299 °C was occurred at a sliding region on the primary shear zone as shown in Fig 16a.

The biggest displacement was achieved about 2.84 mm in total displacement at the end of chip formation (Fig. 16b). The biggest deformation was occurred on the primary deformation zone, followed by the secondary deformation zone. This also causes higher stress occurred in this area, about 3565 MPa in primary shear zone (Fig.16c). These results are agreeable with [31], where the major deformation during cutting process were concentrated in two region close to the cutting tool edge, and the bigger deformation were occurred in the primary deformation zone, followed by secondary deformation zone, sliding region and sticking region.

Fig. 16d shows the highest effective strain occurred on primary shear zone about 5.03 mm/mm, and then followed by secondary shear zone about less than 2.51 mm/mm.

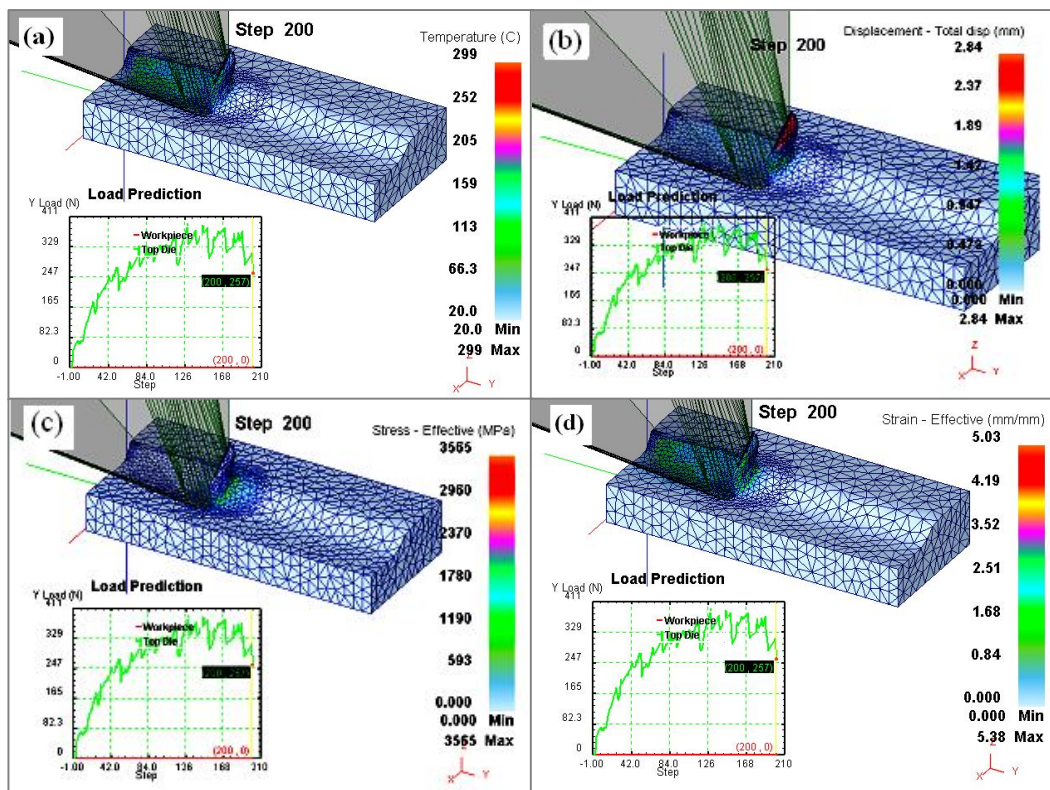


Fig. 16. Simulation results for cutting speed of 200 m/min, rake angle of 20 deg and clearance angle of 5 deg, a) Displacement, b) Effective stress, c) Effective Strain and c) Generated temperature

Fig. 17 shows the sticking area and sliding area at chip formation. In the sticking region, the work piece material adheres to the tool and shear occurs within the chip, the high frictional force caused high temperature generated. Therefore, the highest temperature in the chip occurred in the sliding region (contour of yellow and red color that achieve temperature of 299 °C), followed by sliding areas that only generated temperature under 140 °C (contour of green color).

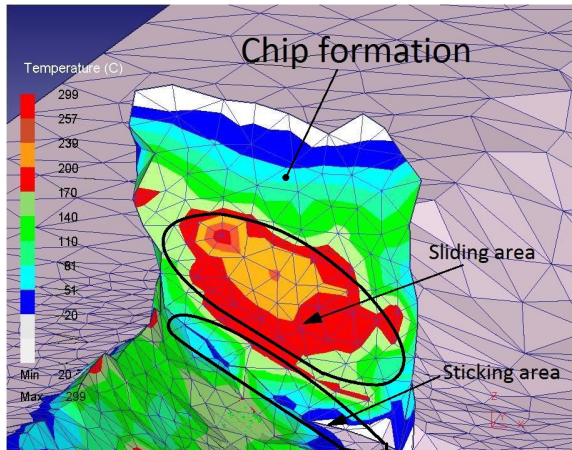


Fig. 17. Sticking and sliding areas in secondary deformation zone

IV. Conclusion

The distribution of cutting force, effective stress and generated temperature obtained from simulations are agreeable with the results given in the literature.

From the simulation results, it can be concluded that by increasing the rake angle (α) in the turning of ductile cast iron using carbide tool, will improves the machining performance, since it will reduces the temperature generated, cutting force, stress, and strain. But, by increasing the clearance angle (γ), it does not has much influence on the temperature generated, cutting force, stress and strain.

For chip formation, in the sticking region, the work piece material adheres to the tool and shear occurs within the chip, the frictional force is high and consequently temperature is generated. Therefore, the highest temperature in the chip usually occurs in the sliding region.

The temperature is an important parameter that controlling the quality of the surface finish, tool wear, and chip segmentation. Controlling the temperature generated is also important in maintaining and controlling the microstructure and hardness at underneath workpiece's surface.

Furthermore, thermal aspects become more important topic with high cutting speeds presently used in industrial processes. Therefore simulation techniques is

recommended to study and evaluate the thermal aspects in metal cutting process.

Acknowledgments

The authors would like to thanks to the Government of Malaysia and National University of Malaysia for their financial support under 03-01-01-SF1214 and UKM-GUP-BTT-07-25-025 Grants.

References

- [1] Barrow, G., A review of experimental and theoretical techniques for assessing cutting temperature, *Annals of the CIRP*, Vol. 22, n. 2, pp.203–211, 1973.
- [2] Seker, U., Korku, I., Turkut, Y., Boy, M. *The measurement of temperature during machining*, International Conference Power Transmission, Ankara, Turkey, 2003.
- [3] Jaharah, A.G., Che Hassan, C. H., Muhamad, N. Machined surface of AISI H13 tools steels when end milling using P10 tin coated carbide tools, *European J. of Scientific Research*, Volume 26, n.2, pp.247–254. 2009.
- [4] Jaharah, A. G., Wahid, S. W., Che Hassan, C. H., Nuawi, M. Z., Mohd Nizam, A. R.. The effect of uncoated carbide tool geometries in turning AISI 1045 using Finite Element Analysis. *European Journal of Science Research*, Vol.28, n.2, pp.271–277, 2009b.
- [5] Jaharah, A. G., Choudhury, I.A., Masjuki, H.H., Che Hassan, C. H.. Surface Integrity of AISI H13 Steel in the End Milling Process, *Int. J. of Mechanical and Materials Engineering (IJMME)*. Vol.4, n.1, pp.88–92, 2009.
- [6] Komanduri, R. and Hou, Z.B., A review of the experimental techniques for the measurement of heat and temperature generated in some manufacturing processes and tribology, *Tribology International*, Vol. 34, pp.653–682, 2001.
- [7] El-Wardany, T.I., Mohamed E. and Elbestawi, M.A. Cutting temperature of ceramic tools in high speed machining of difficult-to-cut materials, *Int. J. of Machine Tools and Manufacture*, Vol. 36, pp.611–634, 1996.
- [8] O'Sullivan, D. and Cotterell, M. Temperature measurement in single turning point, *Journal of Materials Processing and Technology*, Vol. 118, pp.301–308, 2001.
- [9] Muller, B. and Renz, U. Time resolved temperature measurements in manufacturing, *Measurement*, Vol. 34, pp.363–370, 2000.
- [10] Outeiro, J.C., Dias, A.M. and Lebrun, J.L. Experimental assessment of temperature distribution in three-dimensional cutting process', *Journal of Machining Science and technology*, Vol. 8, n. 3, pp.357–376, 2004.
- [11] Ranc, N., Pina, V. and Herve, P. Optical measurements of phase transition and temperature in adiabatic shear bands in titanium alloys', *J. of Physique IV France*, Vol. 10, pp.347–352, 2000.
- [12] Sutter, G., Faure, L., Molinari, A., Ranc, N. and Pina, V. An experimental technique for the measurement of temperature fields for the orthogonal cutting in high speed, *International Journal of Machines Tools and Manufacture*, Vol. 43, pp.671–678, 2003.
- [13] Thompson. B. Count Rumford, *an enquiry concerning the source of heat which is excited by friction*. (London: Phil Trans Royal Soc, 18th edition, 1798, pp 278–287).
- [14] Joule JP. *On the mechanical equivalent of heat*. (London: Phil Trans of the Royal Soc, 70th edition, 1850, pp.61–81)
- [15] Rall DL, Giedt WH. *Heat transfer and temperature distribution in metal cutting tool*. (Trans ASME, 78th edition, 1956, pp.1507–15).

- [16] Boothroyd G. *Photographic techniques for the determination of metal cutting temperatures*. *Journal of Applied Physics*, Vol. 12, pp.238–242, 1961.
- [17] Boothroyd G. *Temperatures in orthogonal metal cutting*, Proceeding Int. Mech Engineering, London, 1963, pp.789–810.
- [18] Schwerd F. *Determination of the Temperature Distribution During Cutting* (Z VDI, 9th Edition, pp.211, 1933).
- [19] Komanduri, R., Hou. Z.B., A review of the experimental techniques for the measurement of heat and temperatures generated in some manufacturing processes and tribology, *Tribology International*, Vol. 34, pp. 653–682, 2001.
- [20] Marusich, T.D., Ortiz, Modeling and Simulation of High-Speed Machining, *International Journal for Numerical Methods in Engineering*, Vol. 38, n.21, pp.3675–3694, 1995.
- [21] Cerenitti A. E., Fallbohmer B. P., Wu C.W.T. & Altan B.T., Application of 2D FEM to Chip Formation in Orthogonal Cutting, *J. of materials Processing Tech.*, Vol.59, pp.169 - 180, 1996.
- [22] Cerenitti. A. E., Lazzaroni.C., Menegardo. L. & Altan. T., Turning Simulation Using a Three-Dimensional FEM Code, *Journal of materials Processing Technology*, Vol.98, pp. 99 - 103, 2000.
- [23] Xie, J. Q., Bayoumi, A.E., & Zbib, H. M., FEA Modelling and Simulation of Shear Localized Chip Formation in Metal Cutting, *J. of Materials Processing Tech.*, Vol.38, pp.1067-1087, 1998.
- [24] Shet, C., Finite Element Analysis of the Orthogonal Metal Cutting Process, *Journal of Materials Processing Technology*, Vol.105, pp.95-109, 2000.
- [25] Jawahir, I. S., *An Intermediary Level Short Course on Machining Process Modelling and Optimization for Improved Productivity* (Machining Research Laboratory Center for Manufacturing, Department of Mechanical Engineering Lexington, USA, 2008).
- [26] Columbus, O.H. , *DeformTM - 3D Machining (Turning) Lab* (Scientific Forming Technologies Corporation, 2007).
- [27] Mackerle, J., Finite Element Analysis and Simulation of Machining: a Bibliography (1976 – 1996), *Journal of Materials Processing Technology*, Vol.86, 17-44, 1999.
- [28] Gunay, M.G., Korkut, I., Aslan, E., and Eker, U.S. Experimental investigation of the effect of cutting tool rake angle on main cutting force, *Jour. of Materials Processing Technology* Vol. 166 (2005), p. 44–49.
- [29] Stephenson. A.A, Agapiou, J.S, *Metal Cutting Theory and Practice*, Marcel Dekker. Inc, New York, 1996
- [30] Trent, E. M., *Metal Cutting* (London: Butterworth - Heinmann Ltd, 1991).
- [31] V. Kalhori, in: *Modelling and Simulation of Mechanical Cutting*, Doctoral Thesis, Institutionen for Maskinteknik, Sweden (2001).

His interest research subject areas are Engineering Science, Manufacturing and Production Engineering, and Cutting Tool Technology. His areas of expertise are in Engineering Science, Manufacturing and Production Engineering, Machining and Metal Cutting Simulation and Advanced Engineering.

Some of the publications related to FEM in machining are: *Application of FEM in Investigating Machining Performance*, 2009-2010, accepted to publish on *Advanced Material Research (AMR)*, International; *Effect of Rake Angle on Stress, Strain and Temperature on the Edge of Carbide Cutting Tool in Orthogonal Cutting Using FEM Simulation*, ITB Journal of Engineering Science, Vol. 42 (2), pp. 179-194, 2010, International; *Optimization of Material Removal Rate, Surface Roughness and Tool Life on Conventional Dry Turning of FCD 700*, Project Leader, 2010, accepted to publish on *International Journal Mechanical and Materials Engineering*. International; *Simulation of Turning Process of AISI 1045 and Carbide Tool Using Finite Element Method*, co-leader, Proceeding of the 7th WSEAS Int. Conf. on CIMMACS '08 (Computational Intelligence, Man-Machine Systems and Cybernetics), Cairo, Mesir, December 2008; *Effect of Rake Angle and Clearance Angle on the Wear of Carbide Cutting*, Project Leader, *Engineering e-Transaction (ISSN 1823-6379)* Vol. 4, No. 1, June 2009, pp 7-13.



² **Jaharah A. Ghani** currently is a lecturer and researcher at the Department of Mechanical and Material Engineering, Faculty of Engineering and Built Environment, National University of Malaysia. She graduated in BEng Manufacturing Systems Engineering from Leeds Polytechnic, UK in 1991. Later, she obtained her MSc degree in Manufacturing System Engineering from Warwick University, UK in 1992. She then completed a PhD in Manufacturing Engineering from the University of Malaya, Malaysia. Her current research interests are machining technology of tool steels, cast iron and aerospace materials.



³ **Che Hassan Che Haron** graduated from the University of Bridgeport, USA with a BS in Mechanical Engineering in 1985 and from the University of Pittsburgh, Pennsylvania, USA with an MS in Mechanical Engineering in 1989. He then completed a PhD in Manufacturing Engineering from Coventry University, UK in 1999. His current research interests are machining technology of tool steel, titanium alloys and EDM.

Authors' information

¹ Hendri Yanda^a

² Jaharah A. Ghani^b

³ Che Hassan Che Haron^c

^ahyanda@eng.ukm.my, ^bjaharah@eng.ukm.my, ^cchase@eng.ukm.my



¹ **Hendri Yanda** was born at Bukit Tinggi, West Sumatera, Indonesia on August 19th, 1970. He graduated his bachelor in 1996 at the Department of Mechanical Engineering, Andalas University, Padang, West Sumatera, Indonesia. After graduation from Andalas University, He was accepted directly as lecturer and researcher at Mechanical Engineering Department, Engineering Faculty, Andalas University, Padang, West Sumatera, Indonesia. He obtained MSc degree in Advanced Engineering/Manufacturing from Engineering Manufacturing, School of Engineering, Engineering Faculty, Sheffield Hallam University, Sheffield, United Kingdom. 2001. Currently, he is a research assistant and PhD student at the Department of Mechanical and Material Engineering, Faculty of Engineering and Built Environment, National University of Malaysia.

International Review of Mechanical Engineering (IREME)

Special Issue on Heat Transfer

Guest Editor-In-Chief

Alina Adriana Minea

Faculty of Materials Science and Engineering
Technical University Gh. Asachi Iasi
Bd. D. Mangeron no.59, Iasi, Romania
aminca@tuiasi.ro
alina.minea@yahoo.com

Guest Editorial Board

Oronzio Manca

Dipartimento di Ingegneria Aerospaziale e Meccanica
Seconda Università degli Studi di Napoli
Via Roma 29, Aversa (CE), Italy
oronzio.manca@unina2.it

Harald Raupenstrauch

Department Metallurgy
Chair of Thermal Processing Technology
University of Leoben
Franz Josef Strasse 18, Leoben, Austria
harald.raupenstrauch@mu-leoben.at

Jennifer Wen

Director of Research, Faculty of Engineering
Kingston University
Friars Avenue, Roehampton Vale, London
j.wen@kingston.ac.uk

International Review of Mechanical Engineering (IREME)

Contents

Guest Editorial Board	209
Aim and Topics of the Special Issue	210
Editorial <i>by Alina Adriana Minna (Guest Editor)</i>	211
Numerical Analysis of a Two-Dimensional Thermal Model for a Car Under Body <i>by Antonio Di Mico, Francesca Fortunata, Orsorio Monaco, Alina A. Minna, Daniele Ricci</i>	213
Optimization of Turbulence and Radiation Models for an Improved Prediction of Non-Premixed Turbulent Flames <i>by C. Pfeiler, C. J. Spijker, H. Raspenstrauch</i>	218
Conduction Calorimetry: Some Remarks in Improved Devices <i>by C. August, J. L. Pellegrina, V. Terra</i>	226
Heat Transfer and Weld Geometry at Electron Beam Welding <i>by Georgij M. Mladenov, Elena G. Kalena, Katia Zh. Vutova</i>	235
Variational Approach to Adaptive Control Design for Distributed Heating Systems Under Disturbances <i>by Vasily V. Savin, Georgij V. Katin, Andreas Raub, Harald Achenane</i>	244
Simulation of Thermal Transfer Process in Cast Ingots at Electron Beam Melting and Refining <i>by Katia Zh. Vutova, Elena G. Kalena, Georgij M. Mladenov</i>	257
Theoretical and Experimental Study on the Thermal Performance of Flat Miniature Heat Pipes Including Rectangular Grooves <i>by S. Masale, J. Masuani, M. B. H. Savi, M. C. Zenghede</i>	266
Enhancement of Solar Thermal Energy Storage Using Phase Change Materials: an Experimental Study at Greek Climate Conditions <i>by Michalis Gr. Vrachopoulos, Maria K. Kankou, Dimitris G. Stambas, Vasilis N. Stamatopoulos, Athanasios F. Ganiotis, Eleftherios D. Kavouranis</i>	279

(continued)



Thermal Modeling of Radiogenic Heating, Conduction, Melting, Metal-Silicate Segregation and Convection in Planetary Sciences <i>by S. Sahjpal</i>	285
Analysis of Temperature Field Inside the Fuel Rod of the VVER 440 Fuel Assembly <i>by Miriana Saikoni, Braxidor Hatada, Vladimir Noias</i>	291
Thermodynamic Analysis and Neural Network Model of Open Cycle Desiccant Cooling Systems with Silica Gel <i>by I. P. Koronaki, E. Ragnokis, T. Kakatsios</i>	298
Passive Control of the Turbulent Flow Over a Surface-Mounted Rectangular Block Obstacle and a Rounded Rectangular Obstacle <i>by K. Ahsan</i>	305
Design Simulation of Filing Sequence and Solidification Time for Cast Metal Matrix Composite by Low Pressure Die Casting <i>by R. S. Taşlık, S. Şahinsoykan, K. K. Mak, A. A. Tajid, M. A. M. Khatir Almar, B. B. T. Hong Tsoh</i>	315
Influence of Manufacturing Method and Interface Activators on the Anisotropic Thermal Behaviour of Copper Carbon Nanofibre Composites <i>by M. Kitizmasit, E. Neubauer, V. Bruner, M. Chiriac, M. Attard</i>	321
Thermal Diffusion Coating of Diamonds for Improved and Reliable Thermal Properties of Metal Diamond Composites <i>by M. Kitizmasit, E. Neubauer, I. Smid, C. Eisenmenger-Sittner, P. Angerer</i>	325
Influence of Heat Transfer on the Thermomechanical Behavior of Shape Memory Alloys <i>by Claire Maria, Ziad Masmou, Wael Zaki</i>	329
Modeling and Simulation of Temperature Generated on Workpiece and Chip Formation in Orthogonal Machining <i>by Hendri Yonda, Jabbar A. Ghani, Che Hassan Che Harau</i>	340
Thermodynamic Analysis and Experimental Evaluation of Active and Passive Sorption Wheels <i>by I. P. Koronaki, E. Ragnokis, T. Kakatsios</i>	349
Effect of the Geometric Shape of the Roof (Type Habitat) on the Natural Convection with the Presence of a Heat Source <i>by E. Benachour, B. Drousi, L. Robmani, B. Melbarki, L. Belloufa, K. Aissouze, B. Louise</i>	355
Computational Study of the Conjugate Heat Transfer and the Wall Conduction Effects in a Horizontal Pipe with Temperature Dependent Properties <i>by K. Chahboub, T. Boufendi</i>	361
Experimental Investigation of Elliptical Cross Section Geometry Wickless Heat Pipe Charged with Distilled Water and Ethanol <i>by Ajit M. Kote, Ratnakar R. Kelkar</i>	369





SCImago
Journal & Country
Rank

EST MODUS IN REBUS
Horatio (Saire 1,1,106)

Home

Journal Rankings

Journal Search

Country Rankings

Country Search

Compare

Map Generator

Help

About Us

Show this information in
your own website

Journal Search

Search query

in

Journal Title

Search

Exact phrase

International Review of Mechanical Engineering

Country: Italy

Subject Area: Engineering

Subject Category:

Category	1999	2000	2001	2002	2003	2004	2005	2006	2007	2008	2009	2010	2011	2012	2013	2014
Mechanical Engineering																

Quartile (Q1 means highest values and Q4 lowest values)

Q3 Q3 Q3 Q3 Q3

Publisher: Praise Worthy Prize, Publication type: Journals, ISSN: 19708742, 19708734

Coverage: 2009-2014

H Index: 10

Charts

Data

SJR indicator vs. Cites per Doc (2y)